de Graaff, L. W. S., Rodés, Á., Pallàs Serra, R., Anders, N. S., Seijmonsbergen, A. C. & De Jong, M. G. G. (2023): [10]Be age datings of Late Würmian erratics from Vorarlberg (Austria) and southern Germany.
inatura – Forschung online, 106: 8 S.
Permalink: www.inatura.at/forschung-online/ForschOn_2023_106_0001-0008.pdf

inatura Forschung online

Nr. 106 - 2023

[10]Be age datings of Late Würmian erratics from Vorarlberg (Austria) and southern Germany

L. W. S. de Graaff †[1], Á. Rodés[2], R. Pallàs Serra[3], N. S. Anders[4], A. C. Seijmonsbergen[5] & M. G. G. De Jong[1,6]

[1] Drs. Leo W.S. de Graaff †, Research Foundation for Alpine and Subalpine Environments (RFASE), Berkenrodestraat 17, 2012 LA Haarlem, The Netherlands.
[2] Dr Ángel Rodés, Universidade de Santiago de Compostela, Facultade de Xeografia e Historia, Praza da Universidade, no 1, 15782 Santiago de Compostela, Spain.
E-Mail: contact@angelrodes.com
[3] Dr. Raimon Pallàs Serra, Department of Earth and Ocean Dynamics, Facultat de Ciències de la Terra, 934035557, Universitat de Barcelona, Spain.
E-Mail: raimonpallas@ub.edu
[4] Dr. Niels S. Anders, Satelligence, Hooghiemstraplein 121, 3514 AZ Utrecht, The Netherlands.
E-Mail: anders@satelligence.com
[5] Dr. Arie C. Seijmonsbergen, Institute for Biodiversity and Ecosystem Dynamics (IBED), University of Amsterdam, Science Park 904, 1098 XH Amsterdam, The Netherlands.
E-Mail: a.c.seijmonsbergen@uva.nl
[1,6] Dr. Matheus G. G. De Jong, Surface and Subsurface Resources, Berkenrodestraat 17, 2012 LA, Haarlem, The Netherlands.
E-Mail: mdejong@susures.nl – Corresponding author.

Abstract

This study presents a [10]Be dataset from Vorarlberg (Austria) and the adjacent Alpine foreland of southern Germany. Out of a total of forty-three samples collected in the field, twenty-five samples of quartz-bearing erratic boulders of Late Würmian age were selected for analyses, measurements and calculations after careful pre-analysis assessment of the sample quality and the potential stratigraphic value. The samples were taken from five localities in Vorarlberg and one locality in southern Germany. The output of fifteen samples passes the threshold in a statistical accuracy assessment. These samples are used in the final determination of the minimum exposure ages. Subsequently, the datings were assessed versus the existing regional morpho- and chronostratigraphic framework, which was erected based on geomorphological and sedimentological data in combination with [14]C age datings. The [10]Be ages at three localities fit in with the stratigraphic framework, while three are considered slightly young or too young when compared with the existing chronologies. The results are considered promising and justify further [10]Be analysis to improve the deglaciation chronology of the area and to find potential calibration sites for cosmogenic surface exposure dating.
Key words: [10]Be age datings, erratic boulders, Vorarlberg, Allgäu, mountains and foreland, Late Würmian

1 Introduction

Dating of landforms and erratics based on cosmogenic [10]Be data has become an established technique in geomorphology and Quaternary stratigraphy (Braumann et al. 2021, 2022; Cockburn & Summerfield 2004; Ivy-Ochs et al. 2007; Kamleitner et al. 2022; Pallàs et al. 2010). A sampling programme for [10]Be age dating was carried out by us in Vorarlberg and southern Germany in the relatively early days of the application of the technique, i. e. in 2006. Results of the analyses and the calculations

Eingereicht: 10.01.2023; Publiziert: 24.01.2023

became available in 2011. The findings remained »on the shelf« for reasons beyond the scope of this paper. They are here presented, not in the least in commemoration of our colleague Leo de Graaff, who deceased in December 2021.

In our study area chronological constraints for the Late Würmian are conventionally based on ^{14}C age datings. Their number, however, is very limited and almost all samples were collected in the foreland (De Jong et al. 2011; Keller & Krayss 2005b; Spötl et al. 2018; Kamleitner et al. 2022). Hence, there was and is a need for additional age datings, not only to refine the local and regional stratigraphy, but also to have a means for linking the inferred climate changes with Northern Hemisphere climate proxies, e. g. Greenland Ice Sheet ice-core data (De Jong et al. 2011).

Geomorphological and glacio-geological research has been carried out in Vorarlberg by the University of Amsterdam since the mid-1950s. The research focus was extended from the primarily glacial-erosive landscape of the mountains of Vorarlberg to the glacial-depositional landscape of the Alpine foreland of southern Germany in the mid-1970s. The investigations resulted in a series of publications on glacial geomorphology and Quaternary stratigraphy. The reader is referred to https://rfase.org/publications-products/ for a comprehensive overview. ESRI Storymap https://bit.ly/vorarlberg-storymap can be consulted for results of the geomorphological mapping.

The deglaciation history of the period following the last major Würmian glacier advance (Preusser 2004; Heiri et al. 2014) is presented in detail by Simons (1985) for the eastern Rhine Valley flank and the Walgau region of Vorarlberg. Similarly, De Jong et al. (1995; https://rfase.org/466-2/) review the deglaciation history of the Vordere Bregenzerwald and the adjacent areas of the Rotach and Weissach valleys in Germany. The morphostratigraphic framework of these areas is tied to that erected for the area of the Argen lobe of the Rhine Glacier in the German foreland (De Jong 1983). Seijmonsbergen (1992) unravels the stratigraphy of the landforms and deposits of the northwestern Rätikon and southern Walgau. A more recent summary of the geomorphological evolution of Vorarlberg is given by de Graaff et al. (2007) and De Jong et al. (2011). We use the stratigraphic scheme of these publications.

Keller & Krayss (2005a, 2005b) present an overview of their geomorphological and stratigraphic research of the entire area of Rhine-Linth Glacier during several decades. Although there are many differences on a local level, their stratigraphic scheme is similar on a regional scale to that of our paper.

Heiri et al. (2014; see also Preusser 2004) review the palaeoclimatic records of the Austrian and Swiss Alps for the period 60-8 ka, and thus present the larger stratigraphic framework for our study. Recently, new age datings have become available in an overview of the entire Rhine and Reuss glacier areas by Kamleitner et al. (2022).

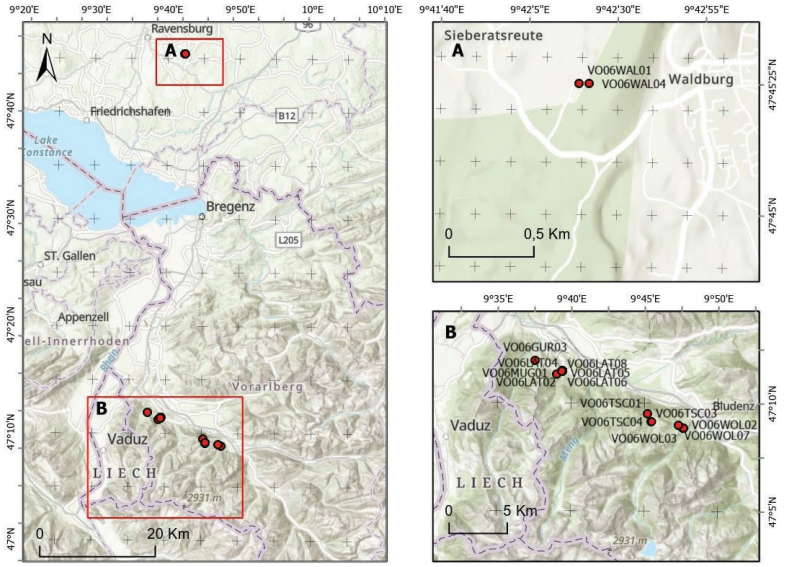

Fig. 1: Sites of samples used in the final determination of the minimum exposure ages. Backdrop maps: »World Topographic Map« and »World Hillshade« from Esri, 2022.

2 Location and sample selection

Samples of erratic blocks were selected on glacial and ice-marginal landforms in Vorarlberg and adjacent Allgäu based on local knowledge of the morphogenetic domains, deposits and stratigraphic position, documented in publications and maps (de Graaff et al. 2007; De Jong 1983; Seijmonsbergen 1992; Simons 1985; https://bit.ly/vorarlberg-storymap; *Fig. 1*). Sampling-site selection in the foreland was aided by cartographic information (»erratic boulder«) from Topographic Sheet 1:25,000 8224 Waldburg (released in 1973). Samples were taken from quartz-bearing boulders (metamorphic rocks; ≈ ≥ 0.5-1 m^3; *Fig. 2*). In most cases, sites were selected where a minimum of four boulders could be sampled which were judged to have been exposed at the surface since deposition by the glacier and lying in situ ever since. To avoid underexposure caused by block rotation or till cover, only boulders were sampled which were well-anchored in late-glacial deposits or lying directly on the stable bedrock surface. Boulders sticking out more than 1 m above the ground were favoured. Core samples with a length of 2 cm were cut by electric drilling in the

boulder surface (*Table A in Appendix*). After careful pre-analysis assessment of the sample quality and the potential stratigraphic value twenty-five samples were selected for ^{10}Be analysis and calculation of exposure ages, out of a total of forty-three samples collected in the field. They are from locations in the lower Ill Valley of Vorarlberg (Gurtis = 4 samples; Tschengla = 4 samples; Latz = 7 samples; St. Wolfgang = 6 samples; Muggabill = 1 sample) and from the Waldburg area in the Alpine foreland (Waldburg = 3 samples). See *Table A in Appendix* for the exact coordinates of the twenty-five selected samples.

Fig. 2: Example of a gneiss erratic at Gurtis.

3 Laboratory treatment, measurements and calculations

Laboratory work was done at the University of Barcelona. Samples were crushed and sieved to extract the 250-1000 µm granulometric quartz fraction. Minerals other than quartz were dissolved by HCl and H_2SiF_6 and remaining quartz grains were cleaned using sequential HF dissolutions to remove any potential atmospheric ^{10}Be (Brown et al. 1991; Kohl & Nishiizumi 1992; Cerling & Craig 1994). Clean quartz cores were then completely dissolved in HF and spiked with 300 µg of ^{9}Be carrier (Bourlès 1988; Brown et al. 1992). Beryllium was separated by successive solvent extractions and alkaline precipitations (*Table A in Appendix*; Bourlès 1988; Brown et al. 1992). Measurements of ^{10}Be concentrations were taken at the ASTER AMS facility in Aix-en-Provence, France (*Table A in Appendix*). The measured ^{10}Be/^{9}Be ratios were corrected for lab procedural blanks and calibrated with the NIST_27900 beryllium standard (Reference Material 4325, assigned value of 2.79 ± 0.03 x 10-11) and using a ^{10}Be half-life of 1.36 ± 0.07 x 106 years (Nishiizumi et al. 2007). Analytical uncertainties are reported as 1σ and include uncertainties associated with AMS counting statistics, standard uncertainty (certification), and chemical blank measurements. ^{10}Be concentration in quartz samples was calculated by following Balco (2006), while the surface exposure ages were calculated with the Cronus online calculator v. 3 (Balco et al. 2008; Balco 2010; *Table B in Appendix*).

^{10}Be measurements were corrected for topographic shielding, to account for the fact that objects are shielded from cosmic radiation by nearby topographic highs and more distant hills and mountains. Commonly, topographic shielding is manually estimated in the field with measurements of local topography and horizon dip angles. We used digital elevation models (DEMs) to automatically calculate topographic shielding for the samples from Vorarlberg. Following Anders (2010), a high-resolution LiDAR (Light Detection And Ranging, 1 m resolution) DEM was used to determine nearby shielding from local topography and a medium-resolution SRTM (Shuttle Radar Topography Mission, resampled to 100 m resolution; Farr et al. 2007) DEM for determining more distant shielding from hills and mountains. The GPS location of each sample location was used as center point from which the maximum horizon dip angles were determined in 360 degrees within 1 km (using the LiDAR DEM) and 50 km (using the SRTM DEM). Shielding corrections were calculated as $\Sigma\alpha_i(1-\mathrm{Sin}^{3.3}\theta)/\Sigma\alpha$, where α_i are the azimuths for the sampling site, and θ are the maximum vertical angles between the sampling and the surface in the α direction.

As the calculations were applied assuming no-erosion conditions and no shielding by snow cover (see Kamleitner et al. 2022), the reported exposure ages can be interpreted as minimum ages of the stabilisation of the deposit (erratic). As a general rule (see Kamleitner et al. 2022), the oldest exposure age of each deposit was considered to be its minimum age. Where the central value of several samples from the same landform overlap with the one-sigma range of the oldest sample in a group, the landform minimum age was computed as the error-weighted mean of the oldest age cluster. Only sample LAT07 yielded a much older age (with no overlap at 2 sigma ranges with the rest of samples from the same landform). It was interpreted as an outlier owing to inheritance, and was not considered in the minimum age determination. The resulting minimum exposure ages based on the constant production rate model for cosmic-ray exposure (*Table B in Appendix*) are: 16.7 ± 0.9 ka for St. Wolfgang, 16.3 ± 0.6 ka for Tschengla, 18.4 ± 1.8 ka for Gurtis, 16.3 ± 0.8 ka for Latz, 18.8 ± 1.2 ka for Waldburg and 16.2 ± 1.5 ka for Muggabill (*Table 1*).

^{10}Be (Lifton et al. 2014)								de Graaff et al. (2007); De Jong (1983); De Jong et al. (1995; 2011)
Sample name	Central value (yr)	External uncertainty (yr)	1/sigma^2	mean/sigma^2	MINIMUM AGE OF LANDFORM (yr)			Morphostratigraphy & accuracy assessment of ^{10}Be mimimum exposure ages (RC = Recessional Complex)
					Weighted mean	External uncertainty		
MUG01	*16172*	*1498*	*4,4563E-07*	*7,21E-03*	***16172***	***1498***	Muggabill	*≈ RC III; age considered slightly young*
TSC02	13726	1355	5,44655E-07	7,48E-03			Tschengla	
TSC03	*15976*	*1160*	*7,4316E-07*	*1,19E-02*	***16275***	***649***		*≈ end RC II; age considered too young*
TSC01	*16217*	*1110*	*8,1162E-07*	*1,32E-02*				
TSC04	*16604*	*1104*	*8,2047E-07*	*1,36E-02*				
WOL06	13831	1568	4,06732E-07	5,63E-03				
WOL01	14555	1856	2,90298E-07	4,23E-03			St. Wolfgang	
WOL04	14564	2030	2,42665E-07	3,53E-03				
WOL03	*16374*	*1245*	*6,4515E-07*	*1,06E-02*	***16740***	***900***		*≈ younger than RC IV; age considered reliable*
WOL02	*16675*	*2285*	*1,9153E-07*	*3,19E-03*				
WOL07	*17366*	*1586*	*3,9755E-07*	*6,90E-03*				
LAT07	23867	2337	1,83098E-07	4,37E-03			Latz	
LAT03	13749	1735	3,32201E-07	4,57E-03				
LAT08	*15408*	*2009*	*2,4777E-07*	*3,82E-03*	***16344***	***779***		*≈ younger than RC IV; age considered reliable*
LAT04	*15567*	*1970*	*2,5767E-07*	*4,01E-03*				
LAT06	*16615*	*1738*	*3,3106E-07*	*5,50E-03*				
LAT05	*16712*	*1359*	*5,4145E-07*	*9,05E-03*				
LAT02	*16874*	*1929*	*2,6874E-07*	*4,53E-03*				
GUR04	15079	1442	4,80916E-07	7,25E-03			Gurtis	
GUR01	15367	1401	5,09476E-07	7,83E-03				
GUR02	16327	1245	6,45151E-07	1,05E-02				
GUR03	*18396*	*1782*	*3,1491E-07*	*5,79E-03*	***18396***	***1782***		*≈ RC II; age considered reliable*
WAL02	16273	1762	3,22098E-07	5,24E-03			Waldburg	
WAL01	*18613*	*1729*	*3,3451E-07*	*6,23E-03*	***18825***	***1159***		*transitional between RC I and II; age considered slightly young**
WAL04	*18998*	*1562*	*4,0986E-07*	*7,79E-03*				

*Age dating of 20.6 ± 1.7 ka for a boulder at Waldburg by Kamleitner et al. (2022) suggests that 18.8 ± 1.2 ka may be slightly young.

in bold and italics: samples contributing to minimum age calculation

Table 1: Minimum ages – error-weighted means and external uncertainties.
The stratigraphic interpretation is displayed in the right column.

4 Stratigraphic interpretation

The minimum ages of the erratics (*Table 1*) have been assessed versus the position of the corresponding landforms and deposits in our regional morpho- and chronostratigraphic scheme (de Graaff et al. 2007; De Jong et al. 2011), which evolved from the work of De Jong (1983) and De Jong et al. (1995).

The Waldburg ridge of the Alpine foreland consists of ice-marginal and predominanty glaciofluvial landforms and deposits formed during the early phases of glacier recession after the last major Würmian advance of the Rhine Glacier. The landforms and deposits are interpreted to be transitional between Recessional Complex (RC) I and RC II. The age of 18.8 ± 1.2 ka is considered to be slightly young. Kamleitner et al. (2022) present ^{10}Be surface exposure ages for boulders from the same locality at Waldburg where we collected our samples: 17.9 ± 0.6 ka (sample RH08) and 20.6 ± 1.7 (sample RH09). Following the rules for handling groups of samples (refer to section Laboratory treatment, measurements and calculations) by combining samples WAL04 and RH09, the minimum exposure age of the landform is 19.7 ± 1.2 ka, which is in line with our chronostratigraphy.

The landforms of Gurtis (Seijmonsbergen et al. 2014: Chapter 5) and Tschengla are among the oldest of a well-developed series of ice-marginal ridges and terraces on the southern flank of the Ill Valley. The age of 16.3 ± 0.6 ka for Tschengla appears too young compared to that of 18.4 ± 1.8 ka for Gurtis. Accepting the latter age dating, these landforms are slightly younger than the above-mentioned landforms and deposits at Waldburg. They are, then, near-synchronous with RC II.

The alluvial-fan terraces at Latz (Seijmonsbergen et al. 2014: Chapter 5) and the ice-marginal features at St. Wolfgang are younger (16.3 ± 0.8 ka and 16.7 ± 0.9 ka, resp.) than the landforms and deposits at Gurtis and Tschengla. In the regional context, they are tentatively interpreted to be younger than the RC IV deposits in the Vordere Bregenzerwald (De Jong et al., 1995; https://rfase.org/466-2/). The minimum exposures ages fit in with this interpretation.

The ice-marginal terrace on top of which the Muggabill boulder rests (Krieg & Verhofstad 1986: pages 78-79), is stratigraphically located between the Gurtis and Latz landforms. The mimimum exposure age of 16.2 ± 1.5 ka must be considered slightly young.

5 Concluding remarks

Application of the technique of dating landforms and erratics based on cosmogenic ^{10}Be data has proven useful in constraining chronologically

the existing stratigraphic scheme. Further application in the study area is considered promising and, hence, recommended. Kamleitner et al. (2022), though, report that few boulders only out a of large number available in their study qualified for surface exposure dating, thus tempering expectations.

Three out of six datings are in line with our stratigraphic scheme. Two ages are slightly young and one too young, the reasons for which remain speculative. Notably useful is the relationship now established over relatively long distance between the foreland cluster of samples of Waldburg and the inner-Alpine samples of the Ill Valley.

Recent work by Braumann et al. (2021, 2022) in high regions of the Silvretta Massif of Vorarlberg, in the catchment of the Rhine Glacier complex, documents the presence of Late Glacial and Early Holocene moraines based on geomorphological studies and ^{10}Be surface exposure datings. These findings support the results of our research in terms of applicability of the technique and of the regional stratigraphy.

6 Acknowledgements

The museum inatura in Dornbirn (Austria) is gratefully acknowledged for its support throughout many years. The LiDAR DEM data of Vorarlberg were kindly made available by Abteilung Geoinformation, Landesamt für Vermessung und Geoinformation (Feldkirch, Vorarlberg).

7 Authors' contributions

L. W. S. de Graaff, who deceased on December 30th, 2021, initiated the research, prepared and carried out the field work and wrote a first draft of the paper. R. Pallàs Serra and Á. Rodés participated in the field work and are responsible for the laboratory analyses and corresponding calculations. N. S. Anders carried out the calculations for topograhic shielding. A. C. Seijmonsbergen provided general support. M. G. G. De Jong participated in the field work, collated all data and coordinated and wrote the final version of the paper.

8 References

Anders, N. S. (2010): Automated calculation of topographic shielding using digital elevation models. – Internal report of the Institute for Biodiversity and Ecosystem Dynamics (IBED), Department of Computational Geo-Ecology, University of Amsterdam.
To be requested via info@rfase.org.

Balco, G. (2006): Converting Al and Be isotope ratio measurements to nuclide concentrations in quartz. – Available at: https://hess.ess.washington.edu (accessed April 2012).

Balco, G. (2010): ^{26}Al – ^{10}Be exposure age/erosion rate calculators: update of constants file from 2.2 to 2.2.1. – Available at: https://hess.ess.washington.edu (accessed April 2012).

Balco, G., Stone, J., Lifton, N. A. & Dunai, T. (2008): A complete and easily accessible means of calculating surface exposure ages or erosion rates from ^{10}Be and ^{26}Al measurements. – Quaternary Geochronology, 3: 174-195. doi: 10.1016/j.quageo.2007.12.001

Bourlès, D. L. (1988): Etude de la géochimie de l'isotope cosmogénique ^{10}Be et de son isotope stable ^{9}Be en milieu océanique. Application à la datation des sediments marins. – Ph.D. Thesis, n° 88 PA11 2026: 246 pp.; Université Paris-Sud, Orsay.

Braumann, S. M., Schaefer, J. M., Neuhuber, S. M., Lüthgens, C., Hidy, A. J. & Fiebig, M. (2021): Early Holocene cold snaps and their expression in the moraine record of the eastern European Alps. – Climate of the Past, 17: 2451-2479. doi: 10.5194/cp-17-2451-2021

Braumann, S. M., Schaefer, J. M., Neuhuber, S. M. & Fiebig, M. (2022): Moraines in the Austrian Alps record repeated phases of glacier stabilization through the Late Glacial and the Early Holocene. – Nature Scientific Reports, 12, 9438: 15 pp. doi: 10.1038/s41598-022-12477-x

Brown, E. T., Edmond, J. M., Raisbeck, G. M., Yiou, F., Kurz, M. D. & Brook, E. J. (1991): Examination of surface exposure ages of Antarctic moraines using in situ produced ^{10}Be and ^{26}Al. – Geochimica et Cosmochimica Acta, 55: 2269-2283. doi: 10.1016/0016-7037(91)90103-C

Brown, E. T., Brook, E. J., Raisbeck, G. M., Yiou, F. & Kurz, M. D. (1992): Effective attenuation lengths of cosmic rays producing ^{10}Be and ^{26}Al in quartz: implications for exposure age dating. – Geophysical Research Letters, 19(4): 369-372. doi: 10.1029/92GL00266

Cerling, T. E. & Craig, H. (1994): Geomorphology and in-situ cosmogenic isotopes. – Annual Reviews of Earth and Planetary Sciences, 22: 273-317. doi: 10.1146/annurev.ea.22.050194.001421

Cockburn, H. A. P. & Summerfield, M. A. (2004): Geomorphological applications of cosmogenic isotope analysis. – Progress in Physical Geography, 28(1): 1-42. doi: 10.1191/0309133304pp395oa

de Graaff, L. W. S., De Jong, M. G. G. & Seijmonsbergen, A. C. (2007): Landschaftsentwicklung und Quartär. – In: Friebe, J. G. (Hrsg.): Vorarlberg. Geologie der Österreichischen Bundesländer: 21-32; Wien (Geologische Bundesanstalt). ISBN 978-3-85316-037-4

De Jong, M. G. G. (1983): Quaternary deposits and landforms of Western Allgaeu (Germany) and the deglaciation after the last major Pleistocene ice advance. – GUA Papers of Geology, 1-18: 186 pp.
Copy available via info@susures.nl

De Jong, M. G. G., de Graaff, L. W. S. & Rupke, J. (1995): Der Eisabbau im Vorderen Bregenzerwald und in den Nachbargebieten (Vorarlberg, Österreich; Bayern, Deutschland) nach dem letzteiszeitlichen Eishochstand. – Jahrbuch der geologischen Bundesanstalt, 138(1): 27-54.
For enclosures: https://rfase.org/466-2/

De Jong, M. G. G., de Graaff, L. W. S., Seijmonsbergen, A. C. & Böhm, A. R. (2011): Correlation of Greenland ice-core isotope profiles and the terrestrial record of the Alpine Rhine glacier for the period 32-15 ka. – Climate of the Past Discussions, 7: 4335-4373. doi: 10.5194/cpd-7-4335-2011

Farr, T. G., Rosen, P. A., Caro, E., Crippen, R., Duren, R., Hensley, S., Kobrick, M., Paller, M., Rodriguez, E., Roth, L., Seal, D., Shaffer, S., Shimada, J., Umland, J., Werner, M., Oskin, M., Burbank, D. & Alsdorf, D. (2007): The Shuttle Radar Topography Mission. – Reviews of Geophysics, 45(2): 33 pp. doi: 10.1029/2005RG000183

Heiri, O., Koinig, K. A., Spötl, C., Barrett, S., Brauer, A., Drescher-Schneider, R., Gaar, D., Ivy-Ochs, S., Kerschner, H., Luetscher, M., Moran, A., Nicolussi, K., Preusser, F., Schmidt, R., Schoeneich, P., Schwörer, C., Sprafke, T., Terhorst, B. & Tinner, W. (2014): Palaeoclimate records 60-8 ka in the Austrian and Swiss Alps and their forelands. – Quaternary Science Reviews, 106: 186-205. doi: 10.1016/j.quascirev.2014.05.021

Ivy-Ochs, S., Kerschner, H. & Schlüchter, C. (2007): Cosmogenic nuclides and the dating of Lateglacial and Early Holocene glacier variations: The Alpine perspective. – Quaternary International, 164-165: 53-63. doi:10.1016/j.quaint.2006.12.008

Kamleitner, S., Ivy-Ochs, S., Manatschal, L., Akçar, N., Christl, M., Vockenhuber, C., Hajdas, I. & Synal, H.-A. (2022): Last Glacial Maximum glacier fluctuations on the northern Alpine foreland: geomorphological and chronological reconstructions from the Rhine and Reuss glacier systems. – Geomorphology, 423 (2023): 26 pp. doi: 10.1016/j.geomorph.2022.108548

Keller, O. & Krayss, E. (2005a): Der Rhein-Linth-Gletscher im letzten Hochglazial. 1. Teil: Einleitung; Aufbau und Abschmelzen des Rhein-Linth-Gletschers im Oberen Würm. – Vierteljahrsschrift der Naturforschenden Gesellschaft in Zürich, 150(1-2): 19-32.

Keller, O. & Krayss, E. (2005b): Der Rhein-Linth-Gletscher im letzten Hochglazial. 2. Teil: Datierung und Modelle der Rhein-Linth-Vergletscherung. Klima-Rekonstruktionen. – Vierteljahrsschrift der Naturforschenden Gesellschaft in Zürich, 150(3-4): 69-85.

Kohl, C. P. & Nishiizumi, K. (1992): Chemical isolation of quartz for measurement of in situ produced cosmogenic nuclides. – Geochimica et Cosmochimica Acta, 56(9): 3583-3587. doi: 10.1016/0016-7037(92)90401-4

Krieg, W. & Verhofstad, J. (Hrsg.) (1986): Gestein und Form. Landschaften in Vorarlberg. – 209 S.; Hard (Hecht).

Lal, D. (1991): Cosmic ray labeling of erosion surfaces: in situ nuclide production rates and erosion models. – Earth and Planetary Science Letters, 104(2-4): 424-439. doi: 10.1016/0012-821X(91)90220-C

Lifton, N. A., Sato, T. & Dunai, T. J. (2014): Scaling in situ cosmogenic nuclide production rates using analytical approximations to atmospheric cosmic-ray fluxes. – Earth and Planetary Science Letters, 386: 149-160. doi: 10.1016/j.epsl.2013.10.052

Nishiizumi, K., Imamura, M., Caffee, M. W., Southon, J. R., Finkel, R. C. & McAninch, J. (2007): Absolute calibration of ^{10}Be AMS standards. – Nuclear Instruments and Methods in Physics Research, Section B, 258(2): 403-413. doi: 10.1016/j.nimb.2007.01.297

Pallàs, R., Rodés, Á., Braucher, R., Bourlès, D., Delmas, M., Calvet, M. & Gunnell, Y. (2010): Small, isolated glacial catchments as priority targets for cosmogenic surface exposure dating of Pleistocene climate fluctuations, southeastern Pyrenees. – Geology, 38(10): 891-894. doi: 10.1130/G31164.1

Preusser, F. (2004): Towards a chronology of the Late Pleistocene in the northern Alpine Foreland. – Boreas, 33(3), 195-210. doi: 10.1111/j.1502-3885.2004.tb01141.x

Seijmonsbergen, A. C. (1992): Geomorphological evolution of an alpine area and its application to geotechnical and natural hazard appraisal in the NW. Rätikon mountains and S. Walgau (Vorarlberg, Austria) (including map series at 1:10,000 scale). – PhD Thesis, University of Amsterdam: 109 pp. https://hdl.handle.net/11245/1.392950

Seijmonsbergen, A.C., De Jong, M. G. G., de Graaff, L. W. S. & Anders, N. S. (2014): Geodiversität von Vorarlberg und Liechtenstein. Geodiversity of Vorarlberg and Liechtenstein. – 304 pp.; Zürich (Bristol-Stiftung) & Bern (Haupt). ISBN 978-3-258-07888-5

Simons, A. L. (1985): Geomorphologische und glazialgeologische Untersuchungen in Vorarlberg, Österreich. – Schriften des Vorarlberger Landesmuseums, Reihe A Landschaftsgeschichte und Archäologie, Bd. I: 165 S.; Bregenz.

Spötl, C., Reimer, P. J. & Göhlich, U. B. (2018): Mammoths inside the Alps during the last glacial period: Radiocarbon constraints from Austria and palaeoenvironmental implications. – Quaternary Science Reviews, 190: 11-19. doi: 10.1016/j.quascirev.2018.04.020

Stone, J. O. (2000): Air pressure and cosmogenic isotope production. – Journal of Geophysical Research. Solid Earth, 105(B10): 23753–23759. doi: 10.1029/2000JB900181

Appendix Table A

Field and laboratory data used to calculate the ^{10}Be exposure ages of erratics from the Ill Valley (Vorarlberg) and in the Alpine foreland (Germany). Names of ^{10}Be samples (standardisation): NIST_Certified. Sample density (2.65 g cm^3) and assumed erosion rate (0 cm yr^{-1}) are similar for all samples.

Field and laboratory data for all samples analyzed								
Sample name	Sample type	Latitude [a] (DD)	Longitude [a] (DD)	Elevation (m) [c]	Sample thickness (cm)	Shielding correction [b]	^{10}Be content [d]	
							atoms g^{-1}	±atoms g^{-1}
WOL01		47.14722	9.79306	762	2.0	0.99060	112380	12644
WOL02		47.14722	9.79361	753 (743.1)	2.0	0.99250	128574	15825
WOL03		47.14722	9.79389	683 (732.1)	2.0	0,99060	118420	5623
WOL04		47.14861	9.79000	782	1.5	0.99250	115120	14470
WOL06		47.14944	9.78806	773	2.0	0.99250	107818	10391
WOL07		47.14944	9.78806	773 (773.6)	2.0	0.99250	136434	9439
TSC01	erratics	47.15806	9.75361	1165 (1155.2)	1.0	0.99700	180240	6155
TSC02	Ill Valley	47.14972	9.76194	1210	2.0	0.99690	156057	12293
TSC03		47.15194	9.75833	1228 (1227.2)	2.5	0.99716	184885	7732
TSC04		47.15167	9.75778	1215 (1222.6)	2.3	0.99700	190577	5716
GUR01		47.19528	9.63556	998	2.0	0.98991	145916	10070
GUR02		47.19528	9.63444	1005	1.0	0.98161	156175	7470
GUR03		47.19861	9.62583	977 (973.7)	2.5	0.99194	172090	13123
GUR04		47.19833	9.62583	984	1.3	0.99194	142467	10653
MUG01		47.18806	9.65028	879 (873.7)	2.7	0.98322	137032	9717
LAT02		47.19000	9.65639	765 (734.8)	1.5	0.98190	130715	12725
LAT03		47.19028	9.65611	748	2.0	0.98691	104280	11579
LAT04		47.19028	9.65611	760 (737.2)	1.0	0.98691	120943	13475
LAT05		47.19028	9.65611	751 (737.5)	1.6	0.98691	128405	7126
LAT06		47.19056	9.65667	752 (730.2)	1.3	0.98691	128086	10998
LAT07		47.19056	9.65667	744	2.7	0.98691	183028	14174
LAT08		47.19056	9.65639	740 (732.2)	2.0	0.98190	116053	13424
WAL01	erratics	47.75694	9.70528	752 (745)	1.5	100.000	146764	10447
WAL02	Alpine	47.75722	9.70500	741	2.7	0.99987	125362	11314
WAL04	foreland	47.75694	9.70611	726	2.1	0.98589	143746	8150

[a] With reference to WGS84 datum

[b] Assuming exponent x = 2.3 in the cosmic ray flux equation : cosx (zenith angle)

[c] Values between parentheses derived from Vorarlberg DEM-2017 (samples used in minimum age calculation) or adjusted using topographic map (WAL01)

[d] Blank values used (ratio ^{10}Be/^{9}Be : 2.41927E^{-15}

Appendix Table B

Exposure ages for constant production rate model. Output from the online exposure age calculator formerly known as the CRONUS-Earth online exposure age calculator v. 3 (Balco et al. 2008), wrapper: 3.0.2; get_age: 3.0.2; muons: 1A, alpha = 1; validate: validate_v3_input.m - 3.0; consts: 2020-08-26 .

Sample name	St (Stone 2000)			Lm (Lal 1991)			LSDn (Lifton et al. 2014)		
	Age (yr)	Interr (yr)	Exterr (yr)	Age (yr)	Interr (yr)	Exterr (yr)	Age (yr)	Interr (yr)	Exterr (yr)
WOL01	14480	1635	1998	14183	1601	1925	14555	1644	1856
WOL02	16670	2060	2448	16267	2010	2354	16675	2061	2285
WOL03	16319	778	1510	15931	759	1420	16374	781	1245
WOL04	14500	1829	2160	14201	1791	2086	14564	1837	2030
WOL06	13736	1328	1718	13483	1304	1652	13831	1338	1568
WOL07	17397	1209	1835	16960	1178	1738	17366	1207	1586
TSC01	16466	565	1423	16069	551	1330	16217	556	1110
TSC02	13861	1096	1552	13607	1075	1485	13726	1085	1355
TSC03	16261	683	1459	15870	666	1368	15976	671	1160
TSC04	16913	509	1435	16489	497	1337	16604	500	1104
GUR01	15475	1072	1630	15127	1048	1548	15367	1065	1401
GUR02	16476	791	1528	16081	772	1436	16327	784	1245
GUR03	18618	1426	2054	18111	1387	1946	18396	1409	1782
GUR04	15164	1138	1656	14837	1114	1577	15079	1132	1442
MUG01	16228	1155	1730	15842	1128	1642	16172	1151	1498
LAT02	16882	1650	2125	16468	1610	2032	16874	1650	1929
LAT03	13638	1519	1865	13391	1492	1800	13749	1532	1735
LAT04	15539	1738	2131	15188	1699	2048	15567	1741	1970
LAT05	16709	931	1620	16305	909	1527	16712	931	1359
LAT06	16612	1432	1946	16214	1398	1856	16615	1433	1738
LAT07	24218	1887	2695	23375	1821	2535	23867	1859	2337
LAT08	15364	1784	2160	15024	1744	2079	15408	1789	2009
WAL01	18703	1338	1998	18230	1304	1894	18613	1331	1729
WAL02	16275	1475	1960	15916	1442	1875	16273	1475	1762
WAL04	19086	1087	1865	18593	1059	1756	18998	1082	1562